24th INTERNATIONAL CONGRESS ON SOUND AND VIBRATION
23–27 July 2017, London

OPTIMIZATION OF EXIT FLOW OF EXPANDING CAVITY WITH A FLOW-EQUILIBRATING DEVICE

Zhang Shiyang

National Key Laboratory on Ship Vibration and Noise, China Ship Development and Design Center, Wuhan, Hubei, China
email: zhangshiyang1987@163.com

Wu Chongjian

National Key Laboratory on Ship Vibration and Noise, China Ship Development and Design Center, Wuhan, Hubei, China

Ding Ziyou

Huazhong University of Science and Technology, Wuhan, Hubei, China

Li Zhaohui

National Key Laboratory on Ship Vibration and Noise, China Ship Development and Design Center, Wuhan, Hubei, China

There are many pipe systems in industry. Noise which is induced by pipe systems is commonly divided into two types: the first noise is so-called flow-induced noise which the impact of current against the wall of a pipe causes the vibration of the wall; the second noise is caused by pressure and velocity fluctuation of the flow at the outlet of pipe. Flow noise at outlet of a pipe accounts for a substantial percentage of total noise of pipe systems. Therefore, it is necessary to install a muffler at the outlet of a pipe for reducing this part of noise.
Expanding muffler is a simple and efficient device. Velocity distribution is uneven when fluid flows into external flow-field from pipe by passing through outlet of expanding cavity, which can cause strong flow noise. This study aims to reduce the largest outlet velocity by designing the flow-equilibrating device in expanding cavity and investigates the influence of different divergence angle on outlet flow noise and flow resistance. Based on the device with divergence angle of 0 degree, numerical method has been used to investigate the influence on acoustic performance (transmission loss) and fluid dynamics performance (energy loss) of devices with different divergence angles. The flow without the flow-equilibrating device is compared with that with the setting device. The simulation results show that the flow velocity with the device has been fully averaged. The concentrating distribution of velocity and pressure fluctuation of the flow at the outlet has been reduced. Thus the goal of noise reduction has been achieved. FVM(Finite Volume Method) has been used to discrete LES turbulence model and FW-H acoustic analogy method has been used to analyze the flow field and acoustic performance of different devices.
Keywords: pipe system, expanding cavity, flow noise, flow-equilibrating device

1. Introduction

Although there were a large amount of literatures on the analysis of severe influence of all kinds of noises on abnormal performance for many apparatus, the noises pollution was still a serious problem in many domains [1-4]. With rapid development of the modern industry, there are many

pipe systems in industry. Noise which is induced by pipe systems can cause many serious problems. So it's important to reduce the sound pressure level of the noise. It's common to install a muffler at the outlet of a pipe to reduce the noise.

In recent decades, the transfer matrix method, finite element method (FEM), boundary element method (BEM) or computational fluid dynamics method (CFD) are widely employed to predict the noise of many pipe systems. The most common calculation method is the transfer matrix method (or four-pole theory) [5]. Ji et al. had used the BEM method to obtain three-dimensional analytical results for several silence configurations which show good agreement with experiments [6-8]. Middelberg et al. had used CFD method to successfully evaluate both the mean flow and acoustic performance of an expansion chamber muffler [9].

In present study, an expanding muffler with flow-equilibrating device is designed. And the influence of different divergence angle on outlet flow noise and flow resistance is investigated. The expanding muffler with flow-equilibrating device is installed at a typical outlet of the ship broadside. This study uses LES turbulence model and FW-H acoustic analogy method to simulate the flow in the expanding muffler..

2. LES Methodologies, FW-H Equation and Energy Loss Equation

2.1 LES Turbulent Model

The incompressible N-S Equation is usually written as Equation 1:

$$\rho\left(\frac{\partial U_i}{\partial t} + U_j \frac{\partial U_i}{\partial x_j}\right) = -\frac{\partial p}{\partial x_i} + \mu\nabla^2 U_i + \rho g_i \tag{1}$$

where $\nabla^2 = \partial^2/\partial x_i^2$ is called the Laplacian and *P* is the pressure.

The basic idea of LES is to compute the dynamics of large energy containing scales of motion as much as is economically feasible while modeling the effects of small motions. The definition of large and small will be achieved through filters. Applying a filtering operation to the N-S equation (Equation 1) and yields an equation governing the filtered velocity field (note that here and henceforth the commutativity of filter and differentiation is assumed):

$$\frac{\partial \overline{u_i}}{\partial t} + \frac{\partial}{\partial x_j}\left(\overline{u_i u_j}\right) = -\frac{1}{\rho}\frac{\partial \overline{p}}{x_i} + \upsilon\frac{\partial^2 \overline{u_i}}{\partial x_j^2} - \frac{\partial}{\partial x_j}\tau_{ij}^s \tag{2}$$

In Equation 2, u_i means the velocity components in *i*, *j* and *k* direction, $\overline{u_i}$ means the filtered average velocity components, $\tau_{ij}^s = \overline{u_i}\overline{u_j} - \overline{u_i u_j}$ is referred to as subgrid-scale stress tensor.

The most commonly and widely used subgrid model is the Smagorinsky Model. According to his research and hypothesis, τ_{ij}^s can be written as:

$$\tau_{ij}^s - \frac{1}{3}\delta_{ij}\tau_{kk} = \upsilon_T\left(\frac{\partial \overline{u_i}}{\partial x_j} + \frac{\partial \overline{u_j}}{\partial x_i}\right) = 2\upsilon_T\overline{S_{ij}} \tag{3}$$

In Smagorinsky Model, it is assumed that:

$$\upsilon_T = (C_s\Delta)^2\sqrt{2\overline{S_{ij}S_{ij}}} \tag{4}$$

In Equation 4, Δ is the length scale which is usually defined as a function of the local gridding. For a uniform mesh, Δ is usually taken to be twice the grid spacing. C_S is a dimensionless constant which is also referred to as the Smagorinsky constant. The value of C_S generally varies from 0.07 to 0.24 depending on the particular fluid flow problem; in this paper, the value of C_S is set to 0.1. When Equation 3 and Equation 4 are substituted into Equation 2, we finally get the N-S equation for LES method:

$$\frac{\partial \overline{u_i}}{\partial t} + \frac{\partial}{\partial x_j}(\overline{u_i u_j}) = -\frac{\frac{1}{\rho}\partial\left(\overline{p} + \frac{\delta_{ij}}{3}\overline{u_k' u_k'}\right)}{\partial x_i} + \frac{\partial}{\partial x_j}\left[(\nu + \upsilon_T)\left(\frac{\partial \overline{u_i}}{\partial x_j} + \frac{\partial \overline{u_j}}{\partial x_i}\right)\right] \tag{5}$$

2.2 FW-H Equation

Lighthill rearranged the Navier–Stokes equations, which govern the flow of a compressible viscous fluid, into an inhomogeneous wave equation, thereby making a connection between fluid mechanics and acoustics. By using Einstein notation, Lighthill's equation can be written as:

$$\frac{\partial^2 \rho'}{\partial t^2} - c_0^2 \nabla^2 \rho' = \frac{\partial^2 T_{ij}}{\partial y_i \partial y_j} \tag{6}$$

in equation: $T_{ij} = \rho u_i u_j - e_{ij} + \delta[(p - p_0) - c_0^2(\rho - \rho_0)]$.

FW-H equation considers the influence of moving solid boundary on the sound.

$$\left(\frac{\partial^2}{\partial t^2} - c_0^2 \nabla^2\right)\left[p' H(f)\right] = \frac{\partial}{\partial t}\left[\rho_0 V_i \frac{\partial f}{\partial x_i}\delta(f)\right] - \frac{\partial}{\partial x_i}\left[p_{ij}\frac{\partial f}{\partial x_j}\delta(f)\right] + \frac{\partial^2}{\partial x_i \partial x_j}\left[T_{ij} H(f)\right] \tag{7}$$

2.3 Energy Loss Equation

Considering the kinetic energy, pressure energy and potential energy of one section surface of the flow, the energy loss in unit time can be written as:

$$\Delta = \int_{A_1}\left(z_1 + \frac{p_1}{\rho g} + \frac{u_1^2}{2g}\right)\rho u_1 g dA_1 - \int_{A_2}\left(z_2 + \frac{p_2}{\rho g} + \frac{u_1^2}{2g}\right)\rho u_2 g dA_2 \tag{8}$$

In this paper, the potential energy is not considered. A_1 surface stands for the inlet surface and A_2 stands for the grille surface .The relationship between flow resistance and energy loss can be written as:

$$f = \frac{\Delta}{vA} \tag{9}$$

v means the velocity of the inlet surface and *A* means the area of the inlet surface.

3. Simulation Model

The expanding muffler with flow-equilibrating device is installed at a typical outlet of the ship broadside. The model of whole computational domain is shown in Fig.1. To simplify the complicated pipe systems of a ship, a length of elbow pipe plus a length of straight pipe are used. The flow goes by the simplified pipe systems and then goes into the silence trunk. At the inlet of the silence trunk, the expanding muffler with flow-equilibrating is installed. The flow goes into the sea by passing through the grille at the outlet of the silence trunk. The silence trunk is a $600 \times 600 \times 800$ mm box. Considering the efficiency and the number of the mesh, the outer flow domain is chosen as $1600 \times 1600 \times 2000$ mm. There are eight baffles in the expanding muffler. Another model is created by changing the divergence angle into 15 degrees.

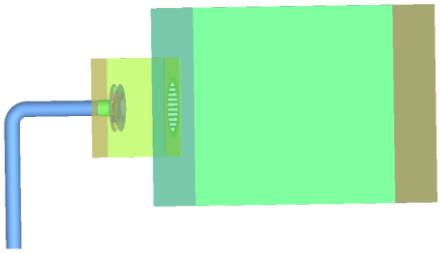

Figure 1: The computational domain

4. Solver and Boundary Conditions

A commercial CFD package, Fluent 16.0 was used. The solver implemented was a coupled implicit solver, with 2nd order implicit time stepping. Second order upwind discretization was used for pressure, momentum, turbulent kinetic energy and the turbulent dissipation rate equations. Coupled pressure velocity is used. The LES turbulence model and the FW-H acoustic analogy method are used to do the study.

As the frequency range between 20 Hz- 1000 Hz is determined to be studied, according to the Sampling Theorem, there is a simple equation between the time step and the obtained biggest frequency.

$$\Delta t = \frac{1}{2mf} \tag{10}$$

m is the written frequency and is commonly set as 1. When f is 1000 Hz, Δt equals 0.0005s. According to the Sampling Theorem, it's better to set a smaller time step to guarantee the reliability of the obtained biggest frequency and the time step is set as 0.0004s.

The boundary condition of the computational domain and the section mesh and the position of origin are shown in Fig.2. The velocity of inlet is 1.811 m/s. The pressure outlet is set at a constant static pressure, in this case atmospheric pressure. Considering that the outer domain is large enough so that it doesn't have any influence on the flow. The side of the outer domain is set as symmetry condition. Other parts are set as no-slip wall condition.

This paper studies the noise which is caused by pressure and velocity fluctuation of the flow at the outlet of pipe. According to the "Fluent 16.0 Users Guide", both the permeable and the impermeable surface are chosen as the source surface. The selected source surface is shown in Fig.3. Considering that the pressure fluctuates little at a short distance, the top surface and the side surface of a cylinder whose radius is 250mm and thickness is 30mm are chosen as permeable source surfaces. The grille surfaces attached to the outer flow domain is chosen as impermeable source surfaces.

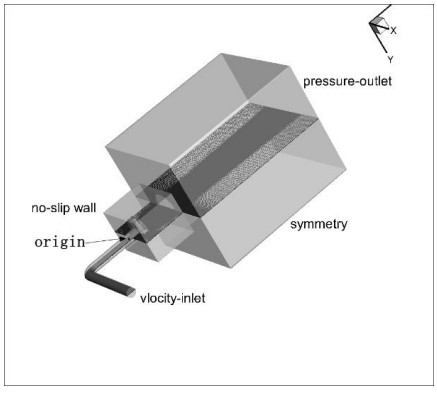

Figure 2: The boundary condition and the section mesh

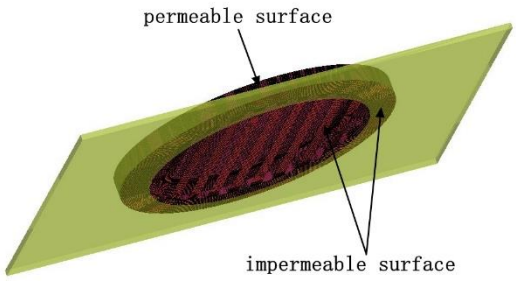

Figure 3: The source surfaces

Before the transient calculation, 2000 iterations of steady calculation is made to get a relatively steady flow field. Before opening the FW-H Acoustics Model, the fluctuating pressure of one point is monitored. As the pressure of the point fluctuates little, the FW-H Acoustics Model can be opened.

5. The Simulation Results

The energy loss of three different calculation models are listed in Table 1. It's shown that when divergence angle is 15 degree, the flow resistance is the biggest.

Table 1: The energy loss of three different models

model-divergence angle	inlet-(total energy)(J/s)	grille-(total energy) (J/s)	energy loss(J/s)	flow resistance(Pa)
mode-0°	43.82	4.13	39.69	1787.34
model-15°	47.79	3.68	44.11	1986.37

Fig.4 and Fig.5 show the velocity contour and the velocity distribution around the expanding muffler and grille at y=0 when divergence angle is 0 degree at one time. Fig.6 and Fig.7 show the velocity contour and the velocity distribution around the expanding muffler and grille at y=0 when divergence angle is 15 degree at one time. Divergence angle can apparently change the flow direction. Fig.8 shows the centerline of the grille. Fig.9 and Fig.10 show the velocity distribution along the centerline of the grille. It's shown that the largest velocity at the outlet of the grille when divergence angle is 15 degree is smaller than that when divergence angle is 0 degree.

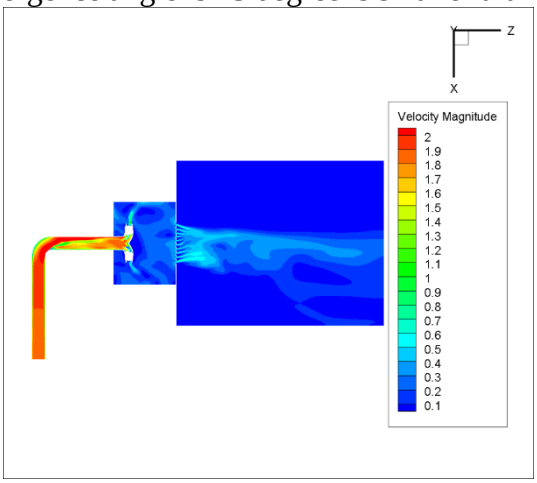

Figure 4: The velocity contour at y=0 when divergence angle is 0 degree

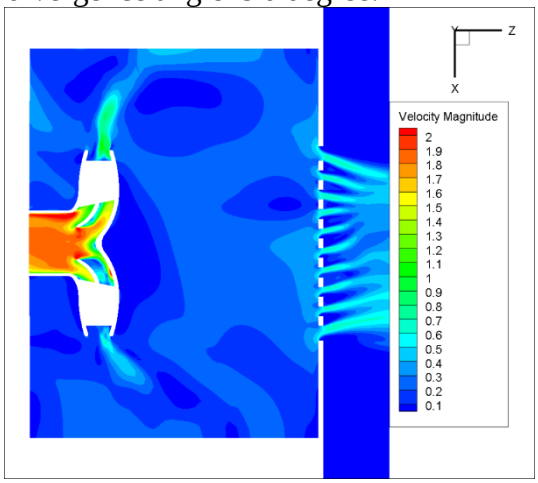

Figure 5: The velocity distribution around the expanding muffler and grille at y=0 when divergence angle is 0 degree

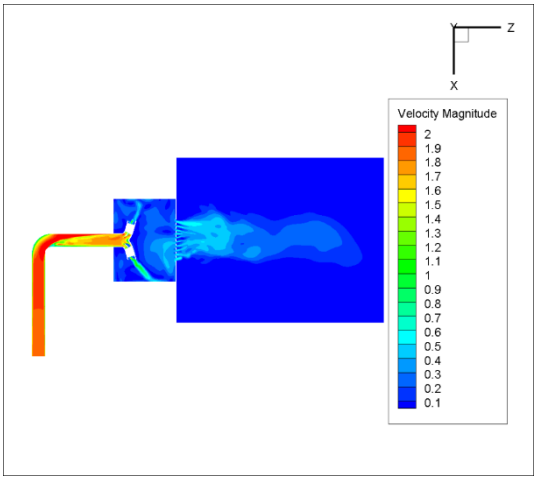

Figure 6: The velocity contour at y=0 when divergence angle is 15 degree

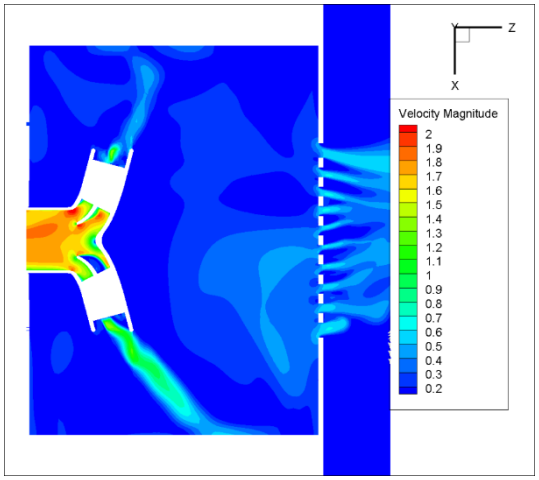

Figure 7: The velocity distribution around the expanding muffler and grille at y=0 when divergence angle is 15 degree

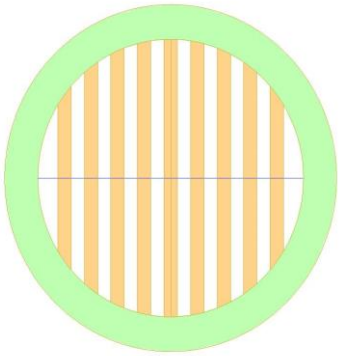

Figure 8: The centerline of the grille.

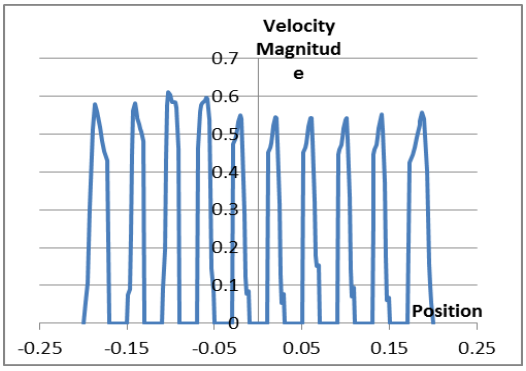

Figure 9: The velocity distribution along the centerline of the grille when divergence angle is 0 degree

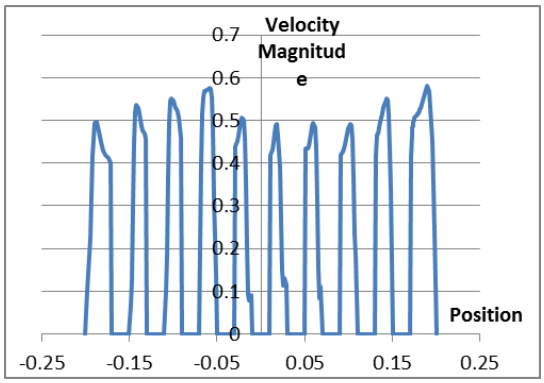

Figure 10: The velocity distribution along the centerline of the grille when divergence angle is 15 degree

This paper compares the overall sound pressure level of the frequency whose range is between 20 Hz- 1000 Hz. The overall sound pressure level of certain range of frequency can be written as;

$$L = 10\lg\left(\frac{L_1}{10} + \frac{L_2}{10} + \cdots\right) \tag{11}$$

$L_1, L_2, \cdots$ are the sound pressure level of the corresponding frequency.

Considering that FW-H is suitable for far-field noise calculation. This paper uses the far-field noise to calculate the near-field noise. The overall sound pressure level of far-field noise and near-field noise can be written as:

$$L_{r_2} - L_{r_1} = 20 \lg (r_1 / r_2) \tag{12}$$

r_1 and r_2 are the distance between the receiver and acoustic source. L_{r_2} and L_{r_1} are the overall sound pressure level of the receivers which are r_2 and r_1 away from the acoustic source.

The position of different receivers is shown in Fig.11. For three different models, the overall sound pressure levels of the certain frequency range (20Hz-1000Hz) at point 3 are compared to compare the acoustic performance.

The sound pressure level spectrum of point 3 of model-0 degree under different frequency ranges is shown in Fig.12. In the XZ plane, 21 receivers are placed. The directivity pattern of overall sound pressure level is shown in Fig.13. The near-field noise has apparent directivity pattern than that of the far-field noise.

The overall sound pressure levels of the certain frequency range of three different models are listed in table 2. It's shown that there are apparent differences between three different models. The overall sound pressure level of model-15 degree is smaller than another model.

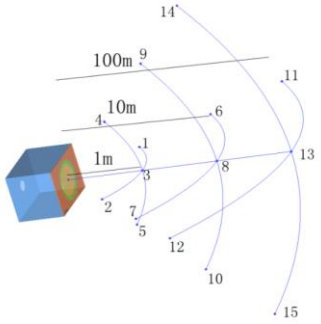

Figure 11: The position of different receivers

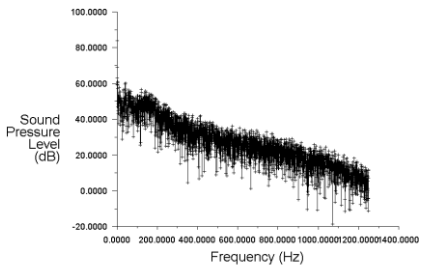

Figure 12: The sound pressure level spectrum of point 3 of model-0 degree under different frequency ranges

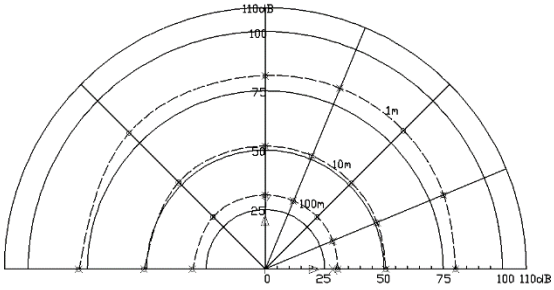

Figure 13: The directivity pattern of overall sound pressure level

Table 2 The overall sound pressure level of three different models.

model-divergence angle	overall sound pressure level(20Hz-1000Hz)
mode-0°	73.57
model-15°	69.97

6. Conclusion

By changing the divergence angle of the muffler, the energy loss and the acoustic performance is different. When divergence angle is 15 degree, the energy loss is bigger than another two models. While the overall sound pressure level is smaller than another two models.

7. Acknowledgement

This work is founded by the National Science Foundation of China under grant numbers 61503354.

REFERENCES

1 Lee M. H., Kang D. B., Kim H. Y., and et al. Classification of Geared Motor Noise Using a Cepstrum and Comb Lifter Analysis, *International Journal of Precision Engineering & Manufacturing*, **8**(3), 45–49, (2007).

2 Jung J. K., Youm W. S. and Park K. H. Vibration Reduction Control of a Voice Coil Motor (VCM) Nano Scanner, *International Journal of Precision Engineering and Manufacturing*, **10**(3), 167–170, (2009).

3 Tran V. H. and Lee S. G. Enhanced wavelet-based methods for reducing complexity and calculation time in sonar measurements, *International Journal of Precision Engineering and Manufacturing*, **10**(2), 31–37, (2009).

4 Wang C., Wu C., Chen L., and et al. A Comprehensive Review on The Mechanism of Flow-induced Noise and Related Prediction Methods, *Chinese Journal of Ship Research*, **11**(1), 57–71, (2016).

5 Munjal M. L. Acoustics of Ducts and Mufflers, 1987.

6 Selamet A., Ji Z. L. and Radavich P. M. Acoustic Attenuation Performance of Circular Expansion Chambers with Offset Inlet/Outlet: II. Comparison with Experimental and Computational Studeis, *Journal of Sound & Vibration*, **213**(213), 619–641, (1998).

7 Selamet A. and Ji Z. L. Acoustic Attenuation Performance of Circular Expansion Chambers with Extended Inlet/Outlet, *Journal of Sound & Vibration*, **223**(2), 197–212, (1999).

8 Ji Z. L. and Selamet A. Boundary Element Analysis of Three-pass Perforated Duct Mufflers, *Noise Control Engineering Journal*, **48**(5), 151–156, (2000).

9 Middelberg J. M., Barber T. J., Leong S. S. and et al. CFD Analysis of the Acoustic and Mean Flow Performance of Simple Expansion Chamber Mufflers, *ASME 2004 International Mechanical Engineering Congress and Exposition*, 151–156, (2004).